# Molecular dynamics study of the density and temperature dependence of bridge functions in normal and supercritical Lennard-Jones fluids

Tapas R. Kunor* and Srabani Taraphder†
*Department of Chemistry, Indian Institute of Technology, Kharagpur 721302, India*
(Received 29 March 2005; revised manuscript received 12 July 2005; published 9 September 2005)

A systematic study of the density and temperature dependence of bridge functions has been carried out using molecular dynamics simulation studies in one-component Lennard-Jones fluids. In deriving the liquid structure, approximate closures are generally used in integral equation theories of liquids to obtain static density correlations. In the present work, we have directly compared the simulated bridge function to two such commonly used closures, viz., hybrid mean spherical approximation (HMSA) [J. Chem. Phys. **84**, 2336 (1986)] and Duh-Henderson [J. Chem. Phys. **104**, 6742 (1996)] closures with thermodynamic parameters varying from the normal liquid to the supercritical fluid phase far from and near the critical point. In the normal liquid region, both closures show a qualitative agreement with the simulated bridge function, although the extent of correlation at distances $\sigma < r \leq 2.5\sigma$ is generally underestimated. A similar behavior is obtained in supercritical fluids far from the critical point where critical fluctuations are no longer important. In contrast, significant deviations are observed in the bridge functions in supercritical fluids near the critical point even at densities as small as 25% or 50% of the critical density. Such behavior appears to have resulted from competing contributions to the bridge function from decreasing indirect correlations and small yet significant cavity correlations persistent even at very low densities.

DOI: 10.1103/PhysRevE.72.031201 PACS number(s): 61.20.Gy, 61.20.Ja, 61.20.Ne

## I. INTRODUCTION

The structure of any homogeneous and isotropic liquid is generally described in terms of the radial distribution function, $g(r)$, or the structure factor, $S(k)$ [1,2]. Several methods have been proposed to calculate the structure of simple liquids, and extensions to molecular as well as multicomponent fluids have been extensively investigated [2]. There has been a recent surge of interest in liquid structure under varying conditions of temperature $T$ and pressure $P$ (or density $\rho$) with the emergence of supercritical liquids as a special class of solvents [3–5]. Liquids under supercritical conditions show unique properties such as (i) enhancement of solvent density around the solute [6–9], (ii) better solvation of organic solutes and high oxidation efficiencies in supercritical water [10], (iii) enhancement of diffusion coefficient and thermal conductivity [4], and (iv) increase in viscosity in a small range of densities and temperatures near the critical point [4]. Supercritical fluids (SCFs) have found vast applications as solvents in chemical reactions ranging from environmentally benign synthesis to several extraction processes, promotion of alternative reaction products, mechanisms, and rates [11]. An accurate understanding of the structure of supercritical fluids is a necessary prerequisite for detailed analysis of these novel properties. Although the structure of a normal liquid is fairly well understood, the effect of large variations in $T$ and $P$ (or $\rho$) especially in SCFs still remains an open question [3].

The goal of the present article is to investigate the static structure of simple liquids with variations in temperature $T$ and density $\rho$. The liquid structure at a given thermodynamic state point may be obtained by using molecular dynamics or Monte Carlo simulation studies [12,13]. However, even with the current availability of computer resources, it may not be computationally possible to explore the structure spanning all relevant regions of the phase diagram. On the other hand, it is well known that the integral equation theories (IETs) of liquid structure and thermodynamics [14] provide a useful alternative to simulation, especially when the structure is investigated for a wide range of $T$ and $P$ (or $\rho$) or if the system poses ergodicity problems. Excluding a small region near the critical point, IETs accurately reproduce the simulated correlations in single phase regions and can also predict most of the liquid-liquid or liquid-gas coexistence lines in several systems [14]. In the region of low-density characteristic of supercritical solvents, the IETs are expected to provide an accurate description of correlations and, hence, appear to offer a convenient route to obtaining the structure in the supercritical region.

Within the framework of IETs, the static correlations in homogeneous isotropic liquids are described in terms of the total correlation function, $h(r)=g(r)-1$, and the direct correlation function, $c(r)$, by solving the Ornstein-Zernike (OZ) equation

$$h(r) = c(r) + \rho_0 \int d\mathbf{r}' c(|\mathbf{r} - \mathbf{r}'|) h(r') \tag{1}$$

in conjunction with an approximate closure relation. $\rho_0$ is the average number density of the liquid. $h(r)$ is related to the interparticle pair potential $\phi(r)$ by the following exact relation [1]:

*Electronic address: tapas@chem.iitkgp.ernet.in
†Electronic address: srabani@chem.iitkgp.ernet.in

 

$$h(r)+1=\exp[-\beta\phi(r)+\gamma(r)+B(r)], \tag{2}$$

where $\gamma(r)=h(r)-c(r)$ is known as the indirect correlation function. As usual, $\beta=(k_BT)^{-1}$, with $k_B$ and $T$ as the Boltzmann constant and absolute temperature, respectively. In Eq. (2), $B(r)$ represents the bridge function that is a sum of an infinite number of integrals involving products, in an increasing order, of correlation functions and simple functions of the potential [14,15]. This series cannot be converted to any usable analytical formula, and in actual practice $B(r)$ has to be approximated by means of additional semiempirical approximations. This is subsequently used to close the numerical solution of Eqs. (1) and (2). However, the approximate closures used in IETs have been developed and tested with the aim of predicting the radial distribution function accurately in the region of high to intermediate densities. Applicability of these closures in the supercritical fluids needs to be addressed carefully before IETs are used to probe liquid structure at low, gaslike densities in the supercritical regions. In this article, our aim is to calculate the bridge function, $B(r)$, a key input to IETs, directly from molecular dynamics simulation of supercritical Lennard-Jones fluids. Closures which accurately predict $g(r)$ in the normal liquid phase of such systems are known and can be compared to the simulated bridge function to assess their applicability in the supercritical region.

Information regarding $B(r)$ may be derived, for example, from a series in powers of the density [16], from implementation of consistency of various thermodynamic properties [17–19]. In this article, we shall focus on the approximate functional forms that have been used to model $B(r)$ in various IETs. At the simplest level, $B(r)$ can be set equal to zero as in the hypernetted chain (HNC) approximation. Alternatively, a local dependence of bridge function on the indirect correlation function $\gamma(r)$ may be assumed as $B=B(\gamma)$. For example, accurate structure and thermodynamics are predicted in hard-sphere fluids by using the semiempirical modified Verlet (MV) closure [20] given by

$$B(r)=\frac{-\gamma^2}{2[1+0.8\gamma]}. \tag{3}$$

In the case of Lennard-Jones fluids, the pair potential is expressed in terms of energy parameter $\epsilon$ and particle diameter $\sigma$ as

$$\phi(r)=-4\epsilon\left[\left(\frac{\sigma}{r}\right)^{12}-\left(\frac{\sigma}{r}\right)^{6}\right]. \tag{4}$$

It has been shown [21] that in such systems, a Weeks-Chandler-Andersen (WCA) partitioning [1] of the potential $\phi(r)$ may be carried out into a soft-core repulsive part, $\phi_R(r)$, and an attractive part, $\phi_A(r)$, by setting

$$\phi_R(r)=\phi(r)-\phi(r_m), \quad r\leqslant r_m,$$

$$=0, \quad r>r_m,$$

$$\phi_A(r)=\phi(r_m), \quad r\leqslant r_m,$$

$$=\phi(r), \quad r>r_m, \tag{5}$$

where $\phi(r)$ exhibits a minimum at $r=r_m$. This is utlized, for example, in the hybrid mean spherical approximation (HMSA) where $B(r)$ is given by [21]

$$B(r)=\ln\left[1+\frac{\exp\{f(r)[\gamma(r)-\beta\phi_A(r)]\}-1}{f(r)}\right]-\gamma(r)+\phi_A(r) \tag{6}$$

with a Roger-Young 'switching' function $f(r)=1-\exp(-\alpha r)$. The parameter $\alpha$ can be varied to impose thermodynamic consistency of the solution. After analyzing the density dependence of the bridge function, Duh and Haymet [22] introduced a semiphenomenological density dependence in the attractive part of the potential that was later modified by Duh and Henderson [23]. When applied to Lennard-Jones fluids, $\phi_A(r)$ takes up the following form [23]:

$$\phi_A(r)=-4\epsilon\left(\frac{\sigma}{r}\right)^6\exp\left[-\frac{1}{\rho^*}\left(\frac{\sigma}{r}\right)^{6\rho^*}\right]. \tag{7}$$

Here, $\rho^*=\rho_0\sigma^3$ is the reduced density of the liquid. It is also assumed that $B(r)\approx B(s)$, where $s(r)=\gamma(r)-\beta\phi_A(r)$ is the indirect correlation function renormalized in terms of $\phi_A(r)$. The resultant expression for the bridge function is free from any adjustable parameter and is given by

$$B(s)=\frac{-s^2}{2\left[1+\left(\frac{5s+11}{7s+9}\right)s\right]}, \quad s\geqslant 0,$$

$$=-\frac{1}{2}s^2, \quad s<0. \tag{8}$$

In the rest of the article, we shall refer to the above equation as Duh-Henderson (DH) closure. The application of HMSA and DH closures in predicting structure, thermodynamics, and vapor-liquid phase equilibria is well documented [14,23]. Several other approximations have been used to model $B(r)$ in Lennard-Jones (LJ) fluids [19,24], soft sphere fluids [25], fused sphere dimeric fluids [26], and several other complex systems [27]. In this article, we shall focus on the applicability of HMSA and DH closures to one-component LJ fluids in the supercritical region.

The accuracy of the approximate closures is usually determined by solving the IET to obtain $g(r)$ and subsequently comparing it to the results of Monte Carlo or molecular dynamics simulation [21–28]. However, a direct calculation of the bridge function and its dependence on the thermodynamic parameters are less frequently investigated. As we shall discuss later, extraction of the bridge function from molecular dynamics or Monte Carlo simulations may require repeated Fourier transformation of correlations to and from the wave vector ($k$) space. An accurate description of the long-range part of $g(r)$ is a necessary prerequisite for this purpose. Several attempts were made earlier to model the large-$r$ part of $g(r)$ [29–31] and ways of elimination of finite-size effects prescribed [32]. In the high-density liquid region, it is found [28] that there exists a highly negative region for

$r \leqslant 1.2\sigma$ followed by an oscillatory decay at the large $r$ remnant of the long-range oscillations of $g(r)$. Recently, a comprehensive analysis of closure relations in binary mixtures of hard-sphere fluids from Monte Carlo simulation studies [33] reveals a breakdown of the assumption of local dependency of $B(r)$ on $\gamma(r)$ either in the region around the first and second neighbor shell or inside the hard core, depending on the system studied. In LJ fluids, the most extensive study of the density and temperature dependence of $B(r)$ has been presented by Llano-Restrepo and Chapman [34], who investigated a range of liquidlike densities from the triple point to supercritical conditions. The overall behavior of $B(r)$ was found to depend strongly on the density of the system. With decreasing density, the negative dip in the core region rapidly becomes shallow and the long-range part structureless after $r > 1.2\sigma$. However, the lowest supercritical density investigated in this work is $\rho^* = 0.4$ at $T^* = 1.5$. In an earlier IET study using second order Percus-Yevick closure [35], the behavior of $B(r)$ of a Lennard-Jones fluid was investigated at densities as low as 0.2. However, the predicted lack of structure in $B(r)$ could not be compared directly with simulations. In the present article, we would like to investigate the nature of the bridge function in one-component Lennard-Jones fluid in the supercritical region with densities $\rho^*$ less than the critical density, $\rho_c^* = 0.29$, at temperatures $T$ near and substantially higher than the critical temperature, $T_c^* = 1.31$.

As the critical point of a fluid is approached, the isothermal compressibility $\chi_T$ diverges as $T$ tends to $T_c$ [36]. Since this divergence occurs smoothly $[\chi_T \sim (1-t)^{-\gamma'}$, where $t = T/T_c$ and $\gamma' = 1.1-1.4]$, there exists a region in the phase diagram for which $\chi_T$ is large and $\chi_T > \chi_T^0$, the compressibility of an ideal gas. A large compressibility near a narrow region around the critical point implies that in this region, large density fluctuations may be sustained without any considerable loss of free energy creating patches of high and low density in the liquid. In spite of the ongoing effort both in theoretical and experimental studies, understanding the structure of the fluid in this compressible regime still remains an open problem. It may be noted that in the compressible region near the critical point, it may become difficult to equilibrate the simulated system because of large volume fluctuations [13]. On the other hand, the presence of substantial density inhomogeneity requires the pair correlations to be described in terms of $g^{(2)}(r_1, r_2, \theta_{12})$, where $\theta_{12}$ is the angle between the vectors $\mathbf{r}_1$ and $\mathbf{r}_2$ [37]. Applications of IETs to derive the structure of simple fluids in the vicinity of the critical point have been investigated where the homegeneity of $B(r)$ is still maintained [38]. In a recent study of attractive supercritical solutions [39], inhomogeneous OZ equations were solved coupled to an inhomogeneous Percus-Yevick closure involving $c(r_1, r_2, \cos(\theta_{12}))$. However, the accuracy of such descriptions needs to be investigated further in detail. Interestingly, insertion of a solute in a supercritical solvent is found to bring out important differences between integral equations [40]. It may be noted that in this article, we shall concentrate primarily on the structure of supercritical LJ fluid away from the critical point assuming the validity of Eq. (1).

We shall next present the method of extraction of the bridge function, $B(r)$, from equilibrated trajectories of a molecular dynamics simulation. The structure of one-component Lennard-Jones (LJ) fluid is determined in both the normal and supercritical regions and the static correlations compared with those predicted by HMSA and DH. It is found that in the subcritical high-density liquid phase and in supercritical fluids far from the critical point, there is a qualitative overall agreement between $B(r)$ obtained from simulation and those obtained from HMSA and DH closures. At intermediate distances, the correlation predicted by the simulation at the level of bridge function is found to be higher than those used in HMSA or DH. In the supercritical region near the critical point, both closures predict a small but smooth change of $B(r)$ from small negative values to zero based on an assumption of homogeneity of the liquid. However, the simulated bridge function seems to provide a qualitatively different behavior in the core region where it starts with a small positive value rapidly changing into near zero values at distances $r \sim \sigma$. This behavior is observed even at densities as small as $\rho_c/2$ and $\rho_c/4$, where the critical fluctuations are normally expected to be of less significance. These deviations are analyzed in terms of the cavity correlation function, $y(r) = g(r)\exp[\beta\phi(r)]$, that is related to the bridge function as

$$B(r) = \ln y(r) - \gamma(r). \tag{9}$$

The relative contributions of $y(r)$ and $\gamma(r)$ to the overall dependence of $B(r)$ on the density of the system are discussed as possible indication of density inhomogeneity at these state points.

The rest of the article is organized as follows. In Sec. II, we outline the method adopted to extract the bridge function and cavity correlation function from molecular dynamics simulation. The results are presented in Sec. III, and Sec. IV concludes with a brief discussion.

## II. METHODOLOGY

As mentioned in the Introduction, we have employed the molecular dynamics simulation method to study the structure of LJ fluid in normal and supercritical regions. Ideally, equilibrium properties of any system may be obtained from Monte Carlo simulation studies. However, we aim at extending later the results of the present study to investigate the correlation between equilibrium structure and the system dynamics. Therefore, molecular dynamics was chosen to be the suitable method. The radial distribution function was calculated by sampling the equilibrated trajectories of particles obtained in a NVE molecular dynamics simulation. The radial distribution function thus simulated may be used to calculate the bridge function in the following way [30,34]. First, $g(r)$ is Fourier-transformed to obtain the structure factor, $S(k)$, as [1]

$$S(k) = 1 + 4\pi\rho_0 \int_0^\infty dr r^2 [g(r) - 1] \frac{\sin(kr)}{kr}, \tag{10}$$

which is related to the Fourier transform of direct correlation function, $\tilde{c}(k)$, as

$$\rho_0 \tilde{c}(k) = 1 - \frac{1}{S(k)}. \tag{11}$$

The next step involves calculation of $\tilde{\gamma}(k)$, the indirect correlation function in the Fourier space, using the following expression:

$$\tilde{\gamma}(k) = \frac{\rho_0[\tilde{c}(k)]^2}{1 - \rho_0 \tilde{c}(k)}. \tag{12}$$

Fourier inversion of $\tilde{\gamma}(k)$ yields $\gamma(r)$, which is finally used to calculate the bridge function as

$$B(r) = \ln g(r) + \beta\phi(r) - \gamma(r). \tag{13}$$

As mentioned earlier, the accuracy of the bridge function thus extracted depends on the range of $r$ over which $g(r)$ has been probed. In earlier studies, the long-range part of $g(r)$ used to be modeled with a suitable ansatz [30]. However, with the advent of large-scale simulation studies with box-lengths larger than 30 Å, such approximate treatments may not be necessary any more. In all the systems investigated here, the conditions were so chosen that $g(r)$ attained its limiting value of unity (with very small fluctuations around it) well within the maximum distances probed. However, in spite of using large systems, it may be difficult to obtain accurate enough statistics at large values of $r$. In addition, even small errors in sampling of large distances may give rise to a substantial accumulation of error in estimating $S(k)$ in the limit $k \to 0$. In practice, we find that estimation of $S(k)$ through $g(r)$ may give relatively large errors in $S(k \to 0)$ especially in low-density supercritical regimes where the large distances are anyway sparsely populated. In the present work, we have extensively compared the wave-vector dependence of $S(k)$ calculated from $g(r)$ and that obtained by direct sampling in the $k$ space [41]. The latter is found to provide a more accurate estimate of $S(k)$ in the small wave-vector limit while both the methods afford nearly indistinguishable values at intermediate to large values of $k$.

It should also be noted that it is not possible to estimate $B(r)$ within the core region (that is, $r < \sigma$) using Eq. (13) as $g(r)$ is zero in this range. Alternatively, one may use Eq. (9) to evaluate the bridge function from the cavity correlation function $y(r)$. The latter may be estimated either using Henderson's equation [42] or employing the direct simulation method of Torrie and Patey [43]. In the present work, we have used Henderson's method, which is known to be accurate at small $r$ [33,34]. In this method, for a system comprised of $N$ particles, the cavity function can be obtained from the following expression [42]:

$$y(r_{12}) = \frac{\exp(\beta\mu^{\mathrm{res}})}{\langle N \rangle} \left\langle N \exp\left[ -\beta \sum_{j>2}^{n+1} \phi(r_{1j}) \right] \right\rangle_{\mu,V,T}, \tag{14}$$

where $\mu^{\mathrm{res}}$ corresponds to the residual chemical potential and the angular brackets represent the grand canonical ensemble average. The above expression can be exactly extended to the canonical ensemble [33] where $N$ remains constant. Therefore, calculation of the cavity correlation function, $y(r_{12})$, amounts to obtaining the average probability of placing a hypothetical test particle (labeled as 1) at a distance $r_{12}$ from any of the $N$ particles labeled as 2. Although computation of this probability is practically free in a NVT Monte Carlo simulation, it can also be evaluated without much computational cost from the equilibrium trajectories generated in MD simulation.

## III. RESULTS AND DISCUSSION

We have carried out both NVE and NVT molecular dynamics (MD) simulations using 864, 5000, and 10000 particles. Periodic boundary conditions are employed to eliminate surface effects. The Verlet neighbor list [44] has been used to optimize the efficiency of the program. In the NVE simulation, we have used the velocity version of the Verlet algorithm to integrate the equation of motion with a time step equal to 1 fs. The system was equilibrated over $10^5$ steps. The radial distribution function $g(r)$ has been calculated by sampling the equilibrated trajectories at an interval of 50 steps during the production run spanning $2 \times 10^5$ steps. The NVE simulation results of LJ fluids have been checked for accuracy against corresponding NVT simulation results of fluids in normal and supercritical regions. The simulation package DL_POLY [45] has been used to generate the trajectories in NVT ensemble using the Nosé-Hoover thermostat [46]. It is found that both NVE and NVT provide nearly identical estimates of $g(r)$. Efficient fast Fourier transform routines have been used to calculate $S(k)$ directly from $g(r)$, and $S(k \to 0)$ is corrected using the direct sampling method in the wave-vector space. $\gamma(r)$ is subsequently calculated by Fourier inversion of $S(k)$. No marked change was obtained by increasing the number of particles from 5000 to 10000, and thus in the rest of the analysis we report results of our simulation using 5000 particles only.

Since Henderson's method is exact in the canonical ensemble, the equilibrated trajectories from our NVT simulation can be used as input to calculate the cavity correlation function, $y(r)$, at small values of $r$. We have also used the equilibrium trajectories from NVE simulation to obtain an approximate estimate of $y(r)$ and hence $B(r)$ at small values of $r$. The canonical ensemble average required to obtain $y(r)$ has been carefully calculated by selecting at least 10 uncorrelated coordinate sets along equilibrium trajectories. For each coordinate set, the test particle was placed at 16 different equally distributed orientations on a grid near each of the 5000 particles present in the system and the cavity correlation was calculated by carrying out a suitable normalization. In both cases, it is well known that estimates of $y(r)$ become statistically unreliable at distances $r \sim \sigma$, and hence $B(r)$ obtained directly from MD is used to represent $B(r)$ at larger distances. $B(r)$ within the core derived from Henderson's method is found to extend smoothly and continuously to $B(r)$ outside the core calculated from the MD simulation.

To facilitate a direct comparison to the simulated bridge function, the approximate functional forms of $B(r)$ as in HMSA or DH have been evaluated using the simulated $\gamma(r)$ as input. In evaluating the HMSA bridge function, the ther-

TABLE I. The states studied in one-component LJ fluid. State I corresponds to the "normal" liquid while state II is in the supercritical region far away from the critical point. States III and IV lie in the low-density supercritical region near the critical point located at $\rho_c^*=0.29$ and $T_c^*=1.31$.

| State | Density, $\rho^*$ | Temperature $T^*$ |
|---|---|---|
| I | 0.8442 | 1.04 |
| II | 0.4221 | 3.95 |
| III | 0.1450 | 1.5 |
| IV | 0.0725 | 1.5 |

modynamic consistency parameter $\alpha$ is obtained by solving the OZ equation with HMSA closure. This value has also been obtained from a fitting equation proposed recently by studying the density and temperature dependence of $\alpha$ [47].

NVE simulation of simple LJ fluids has been extensively reported in the literature, and here we report only the essential details. The length is scaled by the particle diameter $\sigma$ and energy by the LJ energy parameter $\epsilon$. The thermodynamic state of the system is characterized accordingly by the reduced density, $\rho^*=\rho_0\sigma^3$, and the reduced temperature, $T^*=k_BT/\epsilon$. Choosing the mass $m$, diameter $\sigma$, and energy parameter $\epsilon$ to be equal to those characteristic of Ar, time $t$ is found to be scaled by $\tau=\sqrt{m\sigma^2/\epsilon}\sim 2$ ps. We have investigated the structure of the Lennard-Jones fluid at the following regions [48]: (i) the normal liquid of high density, (ii) the supercritical fluid far from critical point, and (iii) the supercritical fluid at densities $\rho_c/2$ and $\rho_c/4$ at a constant temperature near $T_c$. Details of the parameters used are summarized in Table I. As mentioned earlier, we have performed both NVE and NVT simulations at these state points. In the case of NVE results, the temperature reported in the table is an average value calculated from the equilibrated kinetic energy. The equations of motion were integrated using a time step of 1 fs. Although it is definitely possible to use a longer time step in "normal" liquids, the upper limit is found to be about 5 fs in the low-density limit.

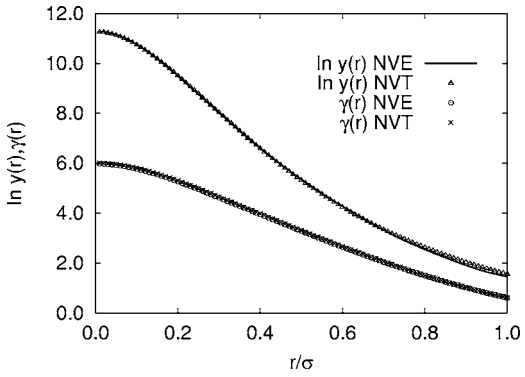


FIG. 1. The indirect correlation function, $\gamma(r)$, and log of the cavity correlation function, $\ln y(r)$, in LJ liquid at $T^*=1.04$ and $\rho^*=0.8442$ (state I of Table I). $\gamma(r)$ obtained using NVE and NVT simulations are represented by open circles and crosses, respectively. $\ln y(r)$ calculated using Henderson's method [42] is shown using solid lines (NVE MD) and triangles (NVT MD).

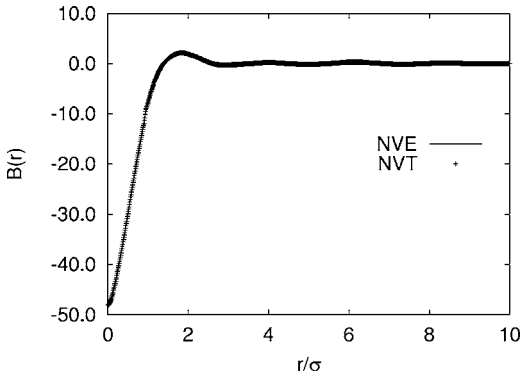


FIG. 2. Comparison of the bridge function, $B(r)$, in the subcritical high-density liquid (state I) from NVE and NVT MD simulation. For distances smaller than $\sigma$, Henderson's method [42] has been employed to evaluate the bridge function.

### A. Normal LJ liquid

In this section, we present the simulated structure of one-component LJ fluid in the homogeneous liquid phase (state I of Table I). The indirect correlation function, $\gamma(r)$, and the cavity correlation function, $y(r)$, are derived from both NVE and NVT MD simulations and the results are presented in Fig. 1. Identical estimates of both of these quantities are obtained, which emphasizes the accuracy of our calculation. The resultant variation of $B(r)$ is shown in Fig. 2. It is found that in the subcritical high-density liquid phase, either of the two methods can be used to obtain quantitatively similar predictions of the bridge function. In Fig. 3, $B(r)$ obtained from NVE simulation has been compared to HMSA and DH closures. As mentioned earlier, we have used the simulated $\gamma(r)$ as input to calculate the approximate closures. To evaluate $B(r)$ using HMSA [Eq. (6)], the value of $\alpha$ is set equal to 0.1272, which produces a thermodynamically consistent solution of the coupled OZ equation at the given state point. Under the given scheme, it is not possible to evaluate numerically the HMSA closure in an intermediate region where $[1/f(r)](\exp\{f(r)[\gamma(r)-\beta\phi_A(r)]\}-1)<-1$. The DH closure produces a better qualitative agreement with the simulated

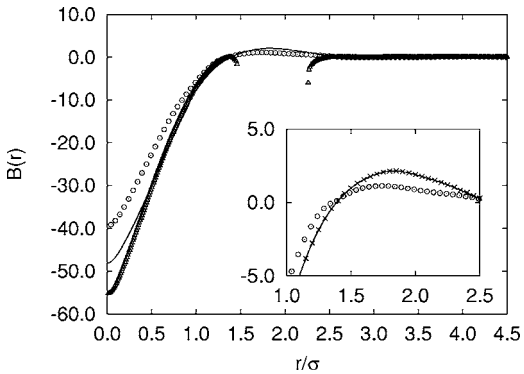


FIG. 3. Comparison of simulated bridge function (NVE, solid line) of LJ liquid in state I with the approximate IET closures, DH (open circle), and HMSA (triangle). The inset highlights stronger correlation predicted by NVE MD (solid line) and NVT MD (×) in comparison to DH.

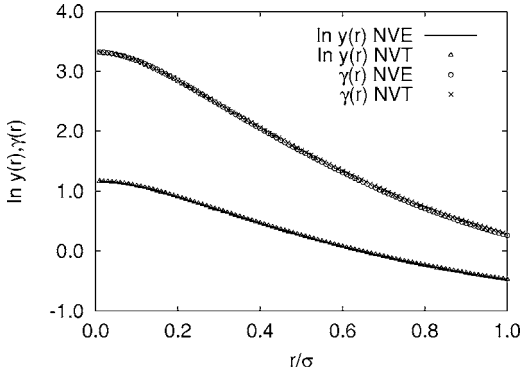


FIG. 4. Indirect correlation function, $\gamma(r)$, and log of cavity correlation function, $\ln y(r)$, at state II with $T^*=3.95$ and $\rho^*=0.4221$. The estimate of $\ln y(r)$ from NVE (solid line) is compared to that obtained from NVT (triangles). $\gamma(r)$ is also obtained from both NVE and NVT MD simulations (square) and are shown by circles and crosses, respectively.

bridge function, although none of the closures seem to represent the short-range behavior accurately. The other important difference appears at around $r\sim 1.2\sigma$. As emphasized in the inset of Fig. 3, larger correlations are predicted by both NVE and NVT simulation results.

### B. Supercritical fluid far from the critical point at high temperatures

In this region, described typically by the state point II in Table I, it is expected that with the decay of critical fluctuations, the system would be more or less homogeneous. Therefore, the positional correlations are supposed to resemble that of a low-density fluid or a gas. The equilibration in this case was done in two stages, initially with a time step of 0.5 fs and then with a time step of 1 fs over $5\times 10^5$ time steps. The production run for each set of initial configuration was carried out over $2\times 10^5$ steps. The results of our simulation are summarized in Figs. 4 and 5. Once again, we have carried out a consistency check using both NVE and NVT simulation results. For the HMSA closure, $\alpha=0.534$. The

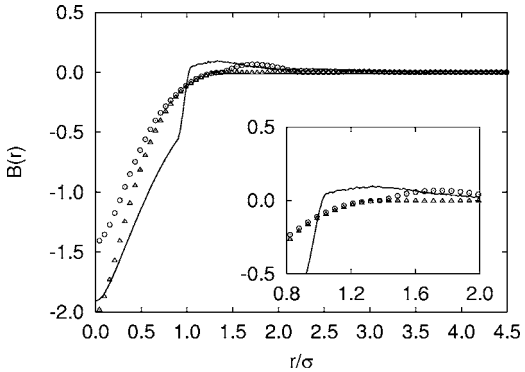


FIG. 5. Comparison of simulated bridge function (from NVT MD, solid line) in LJ SCF far from the critical point at state II with IET closures HMSA (triangle) and DH (open circle). As in Fig. 3, the inset highlights the difference in correlation predicted at intermediate distances.

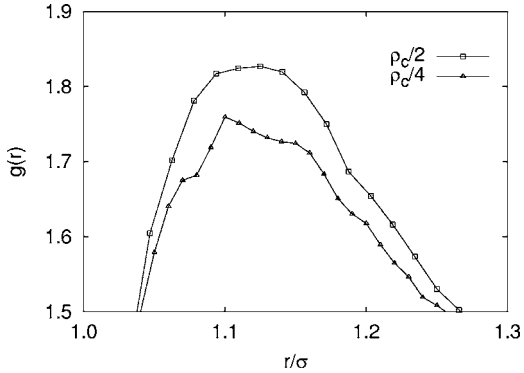


FIG. 6. Comparison of first peak heights of the radial distribution function, $g(r)$, at $T^*=1.5$ and supercritical densities $\rho_c/2$ (squares) and $\rho_c/4$ (triangles) obtained from NVT MD simulation.

state point chosen here lies very close to the Boyle temperature of the fluid [40] and a marked reduction of correlations is expected, as shown in Fig. 4. However, the decrease in $\gamma(r)$ appears to be much more than that observed in $\ln y(r)$, which can probably be attributed to the slow variation of the logarithmic function with variation in density. The overall variation of the bridge function predicted using the NVT simulation qualitatively matches well with the IET closures.

### C. Supercritical fluid at densities $\rho_c/2$ and $\rho_c/4$ near the critical temperature

We have investigated the structure in the low-density supercritical region near the critical temperature at $T^*=1.5$ (states III and IV, see Table I). It is found that decreasing density from $\rho_c$ to $\rho_c/4$ results in a marginal increase in the peak height of $g(r)$ in the region $r\sim\sigma$ from the trajectories of NVE MD simulation. However, as shown in Fig. 6, no such anomaly is observed in the results predicted by NVT MD simulation and, correspondingly, a marginally larger value of $\gamma(r)$ is obtained at $\rho_c/2$ in comparison to $\gamma(r)$ at $\rho_c/4$ (Fig. 7). Otherwise, as expected, $\gamma(r)$ assumes small values and smoothly decays to zero at $r\sim 3\sigma$ (Fig. 7). In Figs. 8 and 9, $\gamma(r)$ and $\ln y(r)$ have been plotted as a function

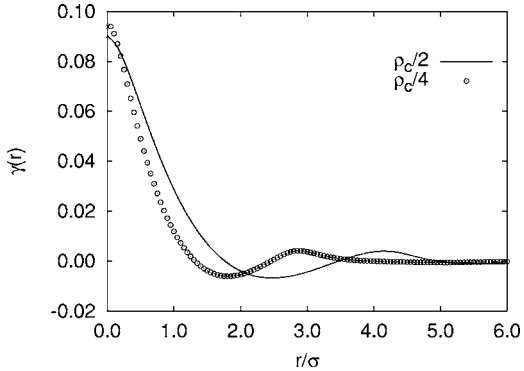


FIG. 7. The indirect correlation function, $\gamma(r)$, of one-component LJ fluid obtained from NVT MD simulation at $T^*=1.5$ and supercritical densities $\rho_c/2$ (solid line) and $\rho_c/4$ (open circles) corresponding to states III and IV of Table I, respectively.

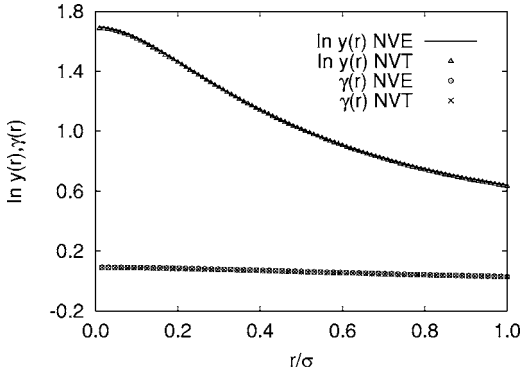


FIG. 8. The indirect correlation function, $\gamma(r)$, and logarithm of the cavity correlation function, $\ln y(r)$, in the supercritical LJ fluid at $T^*=1.5$ and $\rho^*=\rho_c^*/2$ from NVE and NVT MD.

of $r$ for small values of $r$ at these two densities. Our consistency checks show that both NVE and NVT simulations provide nearly identical estimates of $\ln y(r)$ and $\gamma(r)$. We have subsequently used the bridge functions obtained from NVT simulation results at $\rho_c/2$ and $\rho_c/4$ for comparison with the approximate closures, and the results are shown in Figs. 10 and 11, respectively. We have used $\alpha=2.8$ and 4.0 to obtain the HMSA closure at states III and IV, respectively. There is a marked qualitative change in the behavior of $B(r)$ in comparison to the normal liquids (cf. Fig. 2). At distances smaller than $\sigma, B(r)$ no longer exhibits a negative region. This may be understood in terms of the competing contributions of the cavity correlation and the indirect correlation function. With decreasing density, both the correlations have been reduced with a slower variation of $\ln y(r)$ in comparison to $\gamma(r)$. Therefore, a small yet significant effect of cavity correlation persists even at densities as low as $\rho_c/4$ in spite of the indirect correlations becoming smaller in magnitude. At longer distances, $B(r)$ is essentially zero, as expected for such low-density systems. The rapid change in the crossover region $(r\sim\sigma)$ is dominated primarily by $\beta\phi(r)$ as both $\gamma(r)$ and $g(r)$ have small values in this region. The simulated bridge functions thus exhibit significant deviations from the predictions of both HMSA and DH closures in the low-density supercritical region. We have also shown the Duh-Haymet

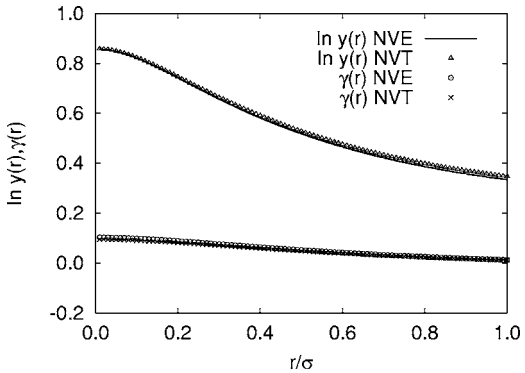


FIG. 9. The indirect correlation function, $\gamma(r)$, and logarithm of the cavity correlation function, $y(r)$, at $T^*=1.5$ and $\rho^*=\rho_c^*/4$ from NVE and NVT MD.

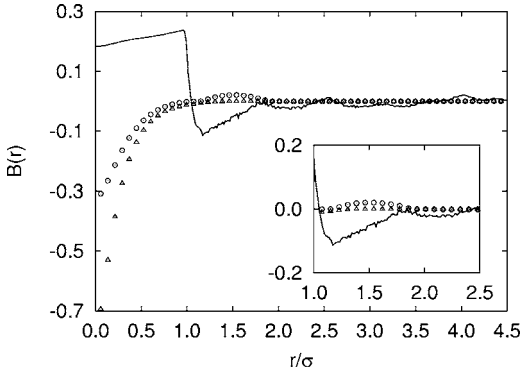


FIG. 10. Comparison of simulated bridge function, $B(r)$, in the supercritical LJ fluid at $T^*=1.5$ and $\rho^*=\rho_c^*/2$ with IET closures. The symbols used are the same as in Fig. 3. $B(r)$ shown has been obtained from NVT MD simulation.

plots to investigate the inter-relationship between the bridge function and the indirect correlation function $\gamma(r)$ or the renormalized indirect correlation function, $s(r)$, in Fig. 12. Qualitatively similar correlations are predicted by the simulated curve and the IET closures both in the homogeneous high-density liquid phase (panel d) as well as in the low-density supercritical fluid far from the critical point (panel c). However, the correlations near the critical point at $\rho_c/4$ and $\rho_c/2$ once again emphasize the breakdown of the assumption of local dependence of $B(r)$ on $\gamma$ or $s$.

## IV. CONCLUSION

In this article, we have presented a molecular dynamics study of the density and temperature dependence of the bridge function in low-density supercritical Lennard-Jones fluids. The results have been compared to approximate closures used in the integral equation theories of liquids. It is found that both HMSA and DH closures provide a qualitatively accurate description of the bridge function in subcritical high density liquids as well as in supercritical fluids far from the critical point. The applicability of these approximate closures to describe the fluid structure hinges mainly on

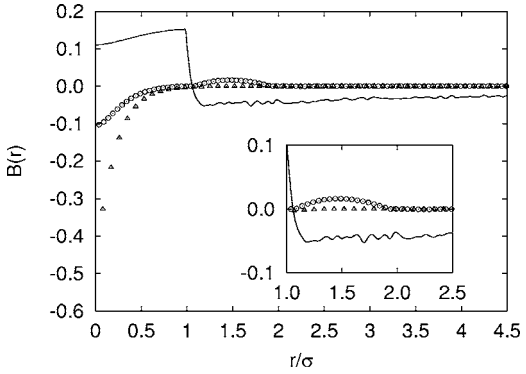


FIG. 11. Comparison of simulated bridge function in the supercritical LJ fluid at $T^*=1.5$ and $\rho^*=\rho_c^*/4$ with IET closures. The symbols used are the same as in Fig. 3. $B(r)$ shown has been obtained from NVT MD simulation.

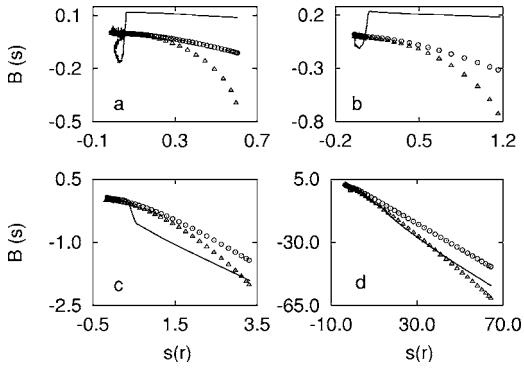


FIG. 12. The Duh-Haymet plot of the bridge function, $B(r)$, vs the renormalized indirect correlation function, $s(r)$, of one-component Lennard-Jones fluid in (a) state IV, (b) state III, (c) state II, (d) state I. The solid line represents results of NVT MD simulation. The circles and triangles correspond to the prediction of DH and HMSA closures, respectively. In the case of HMSA, the bridge function has been plotted as a function of $\gamma(r)$ instead of $s(r)$.

the assumption of homogeneity and isotropy of the system under consideration. An important outcome of the present study is the behavior of cavity correlations at the low-density limit. In this limit, it is expected that cavity correlations should decrease, reflecting the corresponding reduction in direct and indirect correlations. However, at supercritical temperatures close to the critical point, the cavity correlation takes up values that would be otherwise expected at higher densities. This may be attributed to an augmented density in the first neighbor shell of any tagged particle [6,49] in a supercritical fluid. It is found to result in a qualitative change in the overall behavior of the bridge function at small distances even if $B(r)$ remains practically structureless in the region outside the core. Moreover, the local dependence of $B(r)$ on $\gamma(r)$ or $s(r)$ is also altered as shown by regions of nonmonotonic variation of $B(r)$ in Figs. 12(a) and 12(b) at states III and IV. Assumption of such a dependence usually plays a key role in the calculation of properties such as chemical potential [50], which is in turn used in predicting phase equilibria [14,51].

If we focus our attention on the region in the phase diagram near the critical point, it is found that the assumption of a homogeneous, isotropic behavior may lead to erroneous estimates of the correlation. The extent of such an error has been highlighted from our studies of $B(r)$ in supercritical fluid at densities substantially lower than critical density along an isotherm near the critical point. An earlier study of the structure and dynamics of the supercritical fluids [52] indicates the formation of high-temperature clusters, resulting in an inhomogeneous distribution of higher- and lower-density patches throughout the liquid. The dynamics of cluster formation and breaking take place in a relatively fast time scale of about 1 ps [52]. Analysis of our simulated trajectories at states III and IV reveals the existence of high-temperature clusters similar to those observed by Yoshii *et al.* [52]. It therefore appears relevent to extend the IET closures to describe the structural correlations in terms of $h(\vec{r}_1,\vec{r}_2)$ instead. Inhomogeneous PY closure [53] has been recently shown to provide excellent agreement at the level of solute-solvent radial distribution function for a dilute Yukawa solute in supercritical LJ solvent very close to the critical point. However, the inherent limitations associated with PY closures are well documented [14]. Therefore, further investigations are required to address the suitability of extending an existing approximate closure to the inhomogeneous region near the critical point. As it may be a nontrivial exercise to extract the bridge function from simulation in such inhomogeneous systems, a direct test for an appropriate closure still remains an open problem.

## ACKNOWLEDGMENTS

We would like to thank S. Bandyopadhyay, E. Lomba, and G. Pastore for discussions at various stages of this work. Financial support from the Department of Science and Technology (DST), New Delhi is gratefully acknowledged.

[1] J. P. Hansen and I. R. McDonald, *Theory of Simple Liquids*, 2nd ed. (Academic Press, London, 1986).
[2] N. H. March and M. P. Tosi, *Atomic Dynamics in Liquids* (Dover, New York, 1976).
[3] R. Winter and K. Hochgesand, in *High Pressure Molecular Science*, edited by R. Winter and J. Jonas (Kluwer, Dordrecht, 1999); Y. Taniguchi, M. Senoo, and K. Hara, *High Pressure Liquids and Solutions* (Elsevier, Amsterdam, 1994).
[4] T. Clifford, *Fundamentals of Supercritical Fluids* (Oxford, New York, 1999).
[5] *Supercritical Fluids: Fundamentals for Application*, edited by E. Kiran and J. M. H. Levelt-Sengers (Kluwer, Dordrecht, 1993).
[6] S. C. Tucker, Chem. Rev. (Washington, D.C.) **99**, 391 (1999).
[7] I. B. Petsche and P. G. Debenedetti, J. Phys. Chem. **95**, 386 (1991).
[8] O. Kajimoto, Chem. Rev. (Washington, D.C.) **99**, 355 (1999).
[9] W. Song, R. Biswas, and M. Maroncelli, J. Phys. Chem. A **104**, 6924 (2000).
[10] A. A. Chialvo and P. T. Cummings, Adv. Chem. Phys. **109**, 115 (1999).
[11] A. Baiker, Chem. Rev. (Washington, D.C.) **99**, 453 (1999).
[12] M. P. Allen and D. J. Tildesley, *Computer Simulation of Liquids* (Clarendon, Oxford, 1987).
[13] D. Frenkel and B. Smit, *Understanding Molecular Simulation* (Academic Press, San Francisco, 1996).
[14] C. Caccamo, Phys. Rep. **274**, 1 (1996).
[15] Y. Rosenfeld and N. W. Ashcroft, Phys. Rev. A **20**, 1208 (1979).
[16] Y. Zhou and G. Stell, J. Chem. Phys. **92**, 5533 (1992).
[17] A. Vompe and G. Martynov, J. Chem. Phys. **100**, 5249 (1994).
[18] L. L. Lee, J. Chem. Phys. **107**, 7360 (1997).
[19] J. M. Bomont and J. L. Bretonnet, J. Chem. Phys. **114**, 4141 (2001); **119**, 2188 (2003).

[20] L. Verlet, Mol. Phys. **41**, 183 (1980).
[21] G. Zerah and J. P. Hansen, J. Chem. Phys. **84**, 2336 (1986).
[22] D. M. Duh and A. D. J. Haymet, J. Chem. Phys. **103**, 2625 (1995).
[23] D. M. Duh and D. Henderson, J. Chem. Phys. **104**, 6742 (1996).
[24] N. Choudhury and S. K. Ghosh, J. Chem. Phys. **116**, 8517 (2002).
[25] N. Choudhury and S. K. Ghosh, Phys. Rev. E **66**, 021206 (2002).
[26] Y. Duda, L. L. Lee, Y. Kalyuzhnyi, W. G. Chapman, and P. D. Ting, Chem. Phys. Lett. **339**, 89 (2001).
[27] S. M. Kast, Phys. Chem. Chem. Phys. **3**, 5087 (2001).
[28] S. M. Foiles, N. W. Ashcroft, and L. Reatto, J. Chem. Phys. **80**, 4441 (1984).
[29] S. M. Foiles, N. W. Ashcroft, and L. Reatto, J. Chem. Phys. **81**, 6140 (1984).
[30] E. Lomba, M. Alvarez, G. Stell, and J. Anta, J. Chem. Phys. **97**, 4349 (1992); C. Martin, E. Lomba, J. A. Anta, and M. Lombardero, J. Phys.: Condens. Matter **5**, 379 (1993).
[31] S. Kambayashi and J. Chihara, Phys. Rev. E **50**, 1317 (1994).
[32] A. Baumketner and Y. Hiwatari, Phys. Rev. E **63**, 061201 (2001).
[33] R. Fantoni and G. Pastore, J. Chem. Phys. **120**, 10681 (2004).
[34] M. Llano-Restrepo and W. G. Chapman, J. Chem. Phys. **100**, 5139 (1994).
[35] D. Henderson and S. Sokolowski, J. Chem. Phys. **104**, 2971 (1996).
[36] H. E. Stanley, *Introduction to Phase Transition and Critical Phenomena* (Oxford Univ. Press, Oxford, 1987).
[37] P. Attard, J. Chem. Phys. **91**, 3702 (1989).
[38] G. N. Sariskov, J. Chem. Phys. **119**, 373 (2003).
[39] S. A. Egorov, J. Chem. Phys. **116**, 2004 (2002); **112**, 7138 (2000).
[40] A. Perera, J. Chem. Phys. **115**, 6115 (2001).
[41] S. Jorge, E. Lomba, and J. L. F. Abascal, J. Chem. Phys. **116**, 730 (2002).
[42] J. R. Henderson, Mol. Phys. **48**, 389 (1983).
[43] G. Torrie and G. N. Patey, Mol. Phys. **34**, 1623 (1977).
[44] L. Verlet, Phys. Rev. **159**, 98 (1967).
[45] DL_POLY is a package of molecular simulation routines written by W. Smith and T. R. Forester, copyright The Council for the Central Laboratory of the Research Councils, Daresbury Laboratory at Daresbury, Nr. Warrington (1996).
[46] S. Nosé, J. Chem. Phys. **81**, 511 (1984), Mol. Phys. **52**, 255 (1984); W. G. Hoover, Phys. Rev. A **31**, 1695 (1985); **34**, 2499 (1986).
[47] R. Santin, Ph.D. thesis, University of Trieste (2000-2001).
[48] D. M. Heyes, *The Liquid State: Application of Molecular Simulations* (Wiley, New York, 1998).
[49] N. Patel, R. Biswas, and M. Maroncelli, J. Phys. Chem. B **106**, 7096 (2002).
[50] L. L. Lee, J. Chem. Phys. **97**, 8606 (1992).
[51] G. Pastore, R. Santin, S. Taraphder, and F. Colonna, J. Chem. Phys. **122**, 181104 (2005).
[52] N. Yoshii and S. Okazaki, J. Chem. Phys. **107**, 2020 (1997).
[53] S. A. Egorov, J. Chem. Phys. **116**, 2004 (2002).